Shahid Bahonar University of Kerman

Biomechanism and Bioenergy Research

Online ISSN: 2821-1855
Homepage: https://bbr.uk.ac.ir

Iranian Society of Agricultural Machinery Engineering and Mechanization

Modeling and Analysis of a Tractor Diesel Engine Test Stand Structure Using the Finite Element Method

Mohammad Mohammadi[1], Seyed Mohammad Reza Nazemosadat[1]✉, Ahmad Afsari[1]

[1] Department of Mechanical Engineering, Islamic Azad University, Shiraz Branch, Shiraz, Iran.

✉ Corresponding author: smr.nazemosadat@iau.ac.ir

ARTICLE INFO

Article type:

Research Article

Article history:

Received 11 October 2024

Received in revised form 01 November 2024

Accepted 08 December 2024

Available Online 31 December 2024

Keywords:

Detss, abaqus, Inventor, Modal analysis, Static analysis, Fem.

ABSTRACT

The Diesel Engine Test Stand Structure (DETSS) is crucial in industries like automotive, agriculture, shipbuilding, military, and aerospace for engine testing and repair, ensuring safety for technicians. This study designed a steel structure in INVENTOR software, considering the engine's weight, power, and torque. Static and dynamic analyses were conducted using ABAQUS. Static analysis revealed maximum von Mises stress (300–617 MPa) in the motor mount and chassis and minimum stress (100–175 MPa) in the radiator mount, fuel tank, and control panel. Vibrational analysis showed maximum displacement (0.08 mm at 7.20 Hz) in the chassis and mounts, and minimum displacement (0.05 mm at 9.45 Hz) in the control panel, fuel tank, and battery holder. The findings highlight the need for reinforcement and optimization of the motor mount and engine holder.

Cite this article: Mohammadi, M., Nazemosadat, S. M. R., & Afsari, A (2024). Modeling and Analysis of a Tractor Diesel Engine Test Stand Structure Using the Finite Element Method. *Biomechanism and Bioenergy Research*, *3*(2), 75-87. https://doi.org/10.22103/bbr.2024.24161.1090

Publisher: Shahid Bahonar University of Kerman
DOI: https://doi.org/10.22103/bbr.2024.24161.1090

INTRODUCTION

The Diesel Engine Test Stand Structure (DETSS) is a crucial and versatile metallic framework utilized across a range of industries, including automotive, agricultural machinery, shipping, road construction, rail transport, aerospace, and defense. Its importance lies in its role in engine testing and repair, as well as in enhancing technician safety. A primary advantage of this test stand is its cost-effectiveness and the ability to easily control multiple critical parameters of the diesel engine prior to installation and commissioning. This helps identify potential issues in the engine and prevents sudden incidents. The test stand structure provides an effective solution for testing and starting the engine before it is installed in a vehicle. It enables technicians to identify and resolve potential problems, perform final adjustments, and avoid failures due to removal, repair, rebuilding, reinstallation, and adjustments before engine installation.

However, despite its benefits, conventional DETSS has limitations. Current test stands may have more flexibility and comprehensive monitoring capabilities, often resulting in increased time and cost due to the need for repeated assembly and disassembly of the engine to address potential issues. Additionally, they may not fully support real-time diagnostics, which are crucial for identifying and addressing performance issues early in the testing process.

Considering these challenges, this study aims to develop a more advanced and reliable test stand structure that addresses these limitations through innovations in design and diagnostics. Our motivation lies in creating a test stand that minimizes downtime, reduces the need for repeated engine handling, and enhances safety and cost-effectiveness. This study presents a novel test stand design that incorporates enhanced diagnostic capabilities and real-time data collection, enabling technicians to carry out efficient and accurate engine evaluations with minimal adjustments.

Moreover, the stand is equipped with mounts that allow the installation of various types of four, six, and eight-cylinder engines. Additionally, using this stand, the engine can be independently adjusted and installed in forward, backward, and vertical directions (Bogdan et al., 2023). In a universal test stand structure, the housing is directly bolted to the body pattern, making installing automatic or manual transmissions easier, thereby increasing assembly speed. Other advantages of using the DETSS include being designed with wheels for greater stability, easier maneuverability, ease of transport, having a control panel, durability against fatigue tests, quick and hassle-free installation of the engine on designated parts, testing various parameters, speed measurement, engine temperature measurement, oil pressure, and RPM adjustment. This structure also allows for safe and efficient engine testing, repair, and evaluation. Furthermore, with telescopic supports, the DETSS enables the comprehensive testing of various domestic and foreign engines.

In past studies, several DETSS have been developed. For example, (Lloyd & Cackette, 2001) developed a new structure where engine testing processes were analyzed both manually and with computer assistance, enhancing accuracy and reducing testing time. (Voigt, 1991) introduced another test stand focusing on advanced diesel engine simulation, including dynamic modeling and time-delay compensation. This innovation allowed for a more detailed examination of system behaviors, improving durability and control. Similarly, (Altarazi et al., 2020), (Homayounfar & Amiri Chayjan, 2022) and (Reitz et al., 2020) designed test stands emphasizing cost efficiency, ease of transportation, and safety enhancements. While these studies contributed valuable advancements, they only offer a comprehensive solution integrating high-precision diagnostics with ease of operation.

This research aims to address these gaps by designing and analyzing a DETSS with advanced capabilities for real-time monitoring, enhanced safety, and reduced operational costs. Using the

Finite Element Method (FEM) in ABAQUS, our study introduces a flexible and efficient test stand design that can accommodate various engine types with minimal adjustments. This test stand not only improves accuracy and reliability in engine testing but also represents a cost-effective and practical solution for modern industrial needs.

MATERIAL AND METHODS

Modeling of the DETSS in INVENTOR Software

Several DETSS have been designed and manufactured domestically and internationally, optimized for increased static and dynamic strength. Four different models for various applications are shown in Figure 1. These include the American company's model, as shown in Figure 1-a; model T-2680-15, as shown in Figure 1-b; the FlatMax model, as shown in Figure 1-c; and the Bahco 8 model, as shown in Figure 1-d.

Figure 1. Types of DETSS: (a) American Model, (b) T-2680-15 Model, (c) FlatMax Model, (d) Bahco 8 Model.

As shown in Figure 2, the DETSS was modeled using coding based on ISO-2768-mk standards and with the help of Autodesk Inventor 2022 software. This structure consists of nine components: steel chassis, telescopic motor mount holder, telescopic engine holder, radiator holder, radiator pivot arms, battery holder, fuel tank, motor mount pivot arms, and control panel.

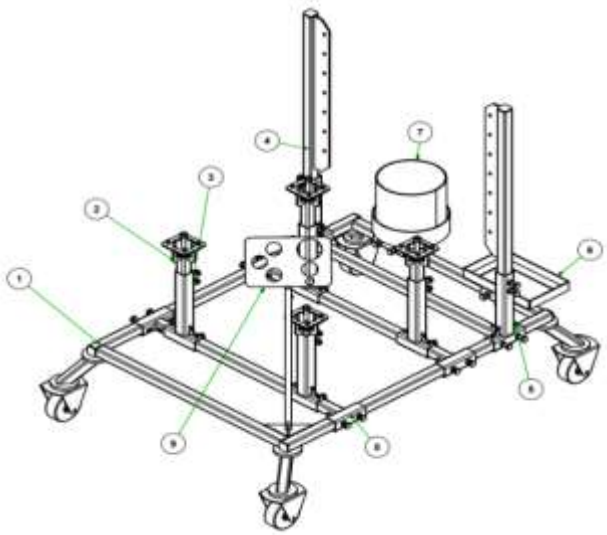

Figure 2. The DETSS under Study: 1) Steel Chassis, 2) Telescopic Motor Mount Holder, 3) Telescopic Engine Holder, 4) Radiator Holder, 5) Radiator Pivot Arms, 6) Battery Holder, 7) Fuel Tank, 8) Motor Mount Arms, 9) Control Panel.

Figures 3-a and 3-b, respectively, show the 3D view of the Cummins DETSS and the side view of the structure in Autodesk Inventor 2022 software, which was studied in this research. In the designed structure, all parts are made of CK45 steel with medium carbon content, commonly used in constructing vehicle chassis and sturdy bodies. This steel has a density of 7830 kg/m³, an elastic modulus of 2.06×10^5 MPa, a Poisson's ratio of 0.3, and yield strength of 414 MPa, which were considered in the mechanical analysis. In the modeled structure, precise measurements of the real structure's dimensions were taken, including the telescopic motor mount holder, radiator holder, battery holder, fuel tank, control panel unit, steel framework, and connecting arms. Table 1 presents the specifications of the components of the DETSS. All dimensions and weights are used in meters and kilograms, and thicknesses are in millimeters in the analyses.

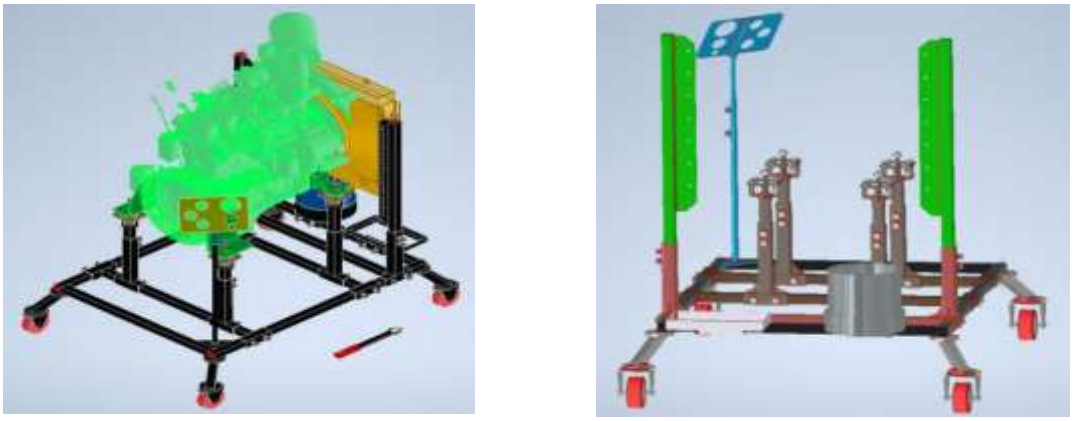

(a) (b)

Figure 3. a) 3D view of the modeled DETSS in Inventor software, b) Side view of the modeled structure in Inventor software.

Table 1. Technical Specifications of the Modeled DETSS Using Inventor Software.

Part name	Dimensional specifications (m)	Weight (kg)	Quantity	Thickness (mm)	Materials
Frame	L1.3×0.04×0.04	5.642	2	4	Ck45
	L0.906×0.04×0.04	3.392	2	4	
Framework	0.906×1.3	30.235	1		Ck45
The final wheel	0.11×0.153	1	4	4	Ck45
Steel wheel	Ø0.04×Ø0.015×0.026	0.163	4		Ck45
Rubber wheel	Ø0.04×0.013		4		Rubber
Axle Wheel Industrial	Ø0.012×0.126	0.106	4		Ck45
Ball bearing roller	DIN-5405-T1 0.01×0.015×0.012		4	10	
Cotter Pin	DIN-6999 0.012×0.008		16		Ck45
The final maintenance structure	DIN-59410 0.04×0.04	0.723	4	4	Ck45
The heel	Ø0.1	0.740	8	12	Ck45
Telescopic-viewing motor	DIN-59410 L0.3×0.04×0.04	1.687	4	4	Ck45
Finger guard-motor	0.036×W 0.06L	0.076	8	8	Ck45
	0.033×W 0.06L	0.065	8	8	Ck45
Engine Handle Rod	Ø0.015×L0.23	0.312	4		Ck45
Rear guard-radiator	DIN-59410 L1×0.04×0.04	4.522	2	4	Ck45
Plate-guard-radiator	L0.75×7×Ø0.012	2.367	2	6	Ck45
Telescopic observation	L0.897×W0.3	8.826	1		Ck45
Cap	0.04×0.04	0.061	6	5	Ck45
Battery holder	DIN-EN-10056 L0.19×0.04×0.04	0.173	2	4	Ck45
Battery maintenance	DIN-EN-10056 L0.32×0.04×0.04	0.291	2	4	Ck45
Wall Tank	L0.761×R0.119	5	1	4	Ck45
Maintenance tank	L0.836×W0.08×R0.131	2.1	1	4	Ck45
	Ø0.262	1.69	1	4	
Axis-dynamic	DIN-59410 L0.15×0.05×0.05×Ø2×0.014	0.657	12	3	Ck45
Control panel	DIN-EN-10060 Ø0.016×L0.6	0.954	1		Ck45
Advanced Control Panel	L0.03×W0.023 R0.015×R0.008	0.014	2	5	Ck45
Page Control Panel	L0.3×W0.02	1.386	1	4	Ck45
Axial Arm	L0.897×W0.15	5.761	2		Ck45
Reinforced telescopic and axial arms	L0.04×W0.04	0.028	25	٥٥	Ck45
Weight Total Construction Maintenance DETSS		232 kg			

Analysis of the DETSS Using the FEM in ABAQUS Software

In this section, the analysis of the DETSS is performed using the FEM. First, the modeled structure is transferred from Inventor software to the finite element software ABAQUS 2022.

Assembly Module and Analysis Settings in ABAQUS for DETSS

Each model in ABAQUS may consist of various components, and the assembly module is used to arrange these components together, forming a complete system and applying geometric constraints between them. Selecting the appropriate solver for model analysis is also crucial. The solver must be capable of performing both the static analysis of the model and the diesel engine and the study of vibrations caused by the engine's dynamics. In this regard, the STATIC GENERAL option from the step module is used to conduct the static analysis with a time step of one second (Gholami et al., 2023). Additionally, the ultimate goal of using ABAQUS software is to obtain and analyze accurate output data. For this purpose, the step module is configured to provide results related to stress, strain, displacement, and frequencies as output data at the end of the analysis.

Support Conditions and Load Application in ABAQUS

In Figure 4, the main boundary and support conditions on all four sides of the steel frame are shown in red, indicating stability in the three main directions with values of U1, U2, and U3, as well as rotational constraints UR1, UR2, and UR3, all set to zero. These boundary conditions are defined by the X-REFERENCE POINT to ensure structural stability under varying loads.

According to the methodologies reviewed by (Bogdan et al., 2023), both dynamic and static loading on the DETSS were considered, including forces resulting from the electric motor’s torque and the inertial forces of the crankshaft and piston system. These loads were analyzed using finite element simulations to ensure the safety and stability of the test stand structure under different experimental conditions.

Figure 4. Boundary and Support Conditions of the Structure in the Load Module in ABAQUS Software.

Figure 5 shows the magnitude and location of the forces applied to the entire DETSS, including the telescopic motor mount holder, radiator and battery holders, tank, control panel plate, steel frame, and pivot arms, which have been entered into ABAQUS software. In Table 2, the values of the concentrated forces applied to the structure, such as those on the battery, fuel tank, radiator, and motor mount holders, are provided in N, with appropriate loadings applied to them.

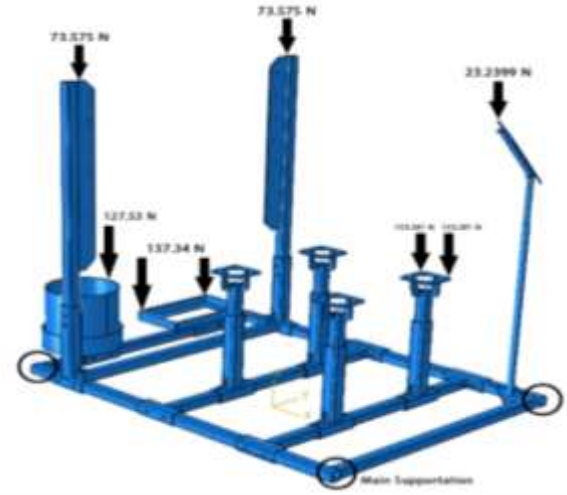

Figure 5. Main Supports and Applied Forces on the Structure in Newtons.

Table 2. The magnitude of Concentrated Compressive Loads on the Structure.

Parts	Newton (N)	Parts	Newton (N)
Battery holder	137.34	Reservoir holder	127.53
Control panel holder	23.23	Engine handle holder	2452.5
Radiator holder	147.15		

Mesh Settings for the Structure in ABAQUS

Two types of elements from the ABAQUS software library were used for the meshing of the structure: pyramidal and cubic elements. The quadratic tetrahedral element (C3D10), a second-order, 10-node, three-dimensional tetrahedral element, was used with 29,991 elements. The linear tetrahedral element (C3D4), a 4-node, three-dimensional hexahedral element, was also used with 903 elements. The overall meshing of the structure consisted of 30,894 elements and 62,662 nodes. As shown in Figure 6, the mesh convergence (validation) of the DETSS reaches a higher accuracy level with 70,000 elements, and according to this figure, with an increase in the number of elements (finer meshing), the stress converges to a constant limit (Nazemosadat et al., 2022). As we approach the regions and areas with maximum von Mises stress, the precision of the analysis decreases. Figure 7 shows the meshing module of the DETSS in ABAQUS software.

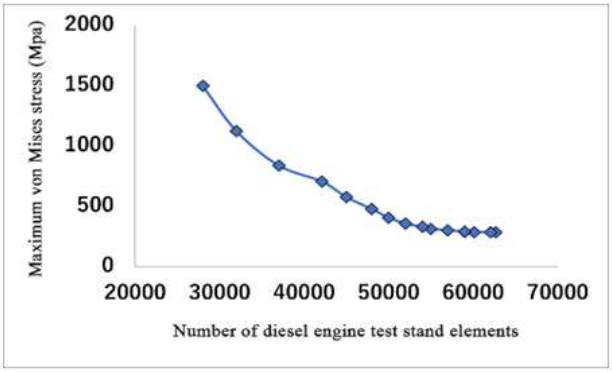

Figure 6. Mesh Convergence of the DETSS.

Figure 7. The meshing of the Structure in the Mesh Module in ABAQUS Software.

RESULTS AND DISCUSSION

Results of the Static Analysis

In all the analyses conducted in this study, a Poisson's ratio of 0.3 was used. This analysis's selected DETSS has a load-carrying capacity of 250 kg, equivalent to 2452.5 N. In Figure 8, the von Mises stress contour is shown in MPa. The maximum von Mises stress occurs in the motor mounts and the telescopic part of the structure, with a value of 617 MPa.

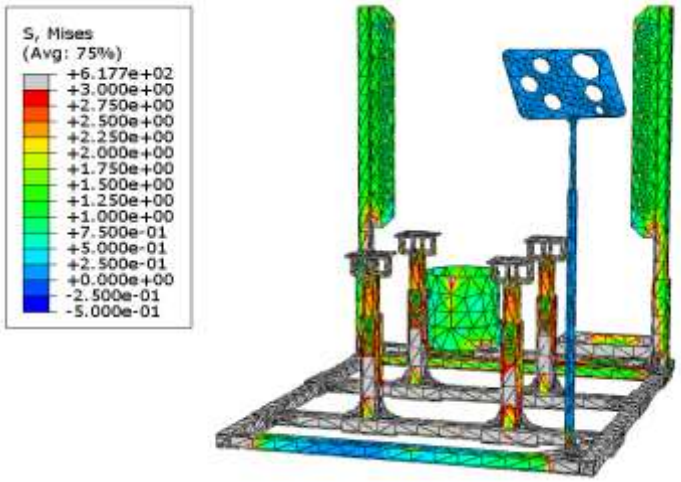

Figure 8. Von Mises Stress Contour Analysis of the DETSS.

Figure 9 - Contour of the Stress Analysis Path for Von Mises Stress in the Motor Mounts of the Structure. Based on the number of nodes, the maximum von Mises stress in the area of the motor mounts to the holder plates ranges between 250 and 300 MPa.

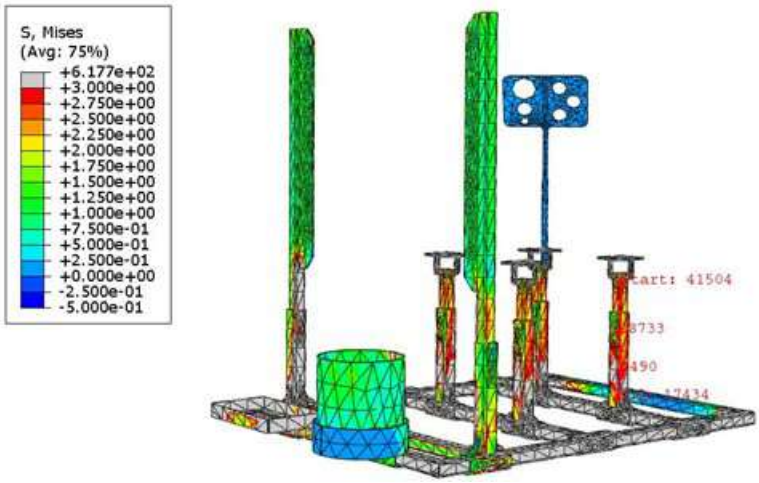

Figure 9. The contour of the Stress Analysis Path for Von Mises Stress in the Motor Mounts of the Structure.

Figure 10 - Contour Path Diagram of the Von Mises Stress Analysis in the DETSS Motor Mounts. The initial stress at node 41504 is approximately 200 MPa, with a descending path initially until it reaches the second node 28733. After that, the stress increases, continuing to the third node, 4490, and decreasing again. The maximum stress occurs at the third node, around 300 MPa.

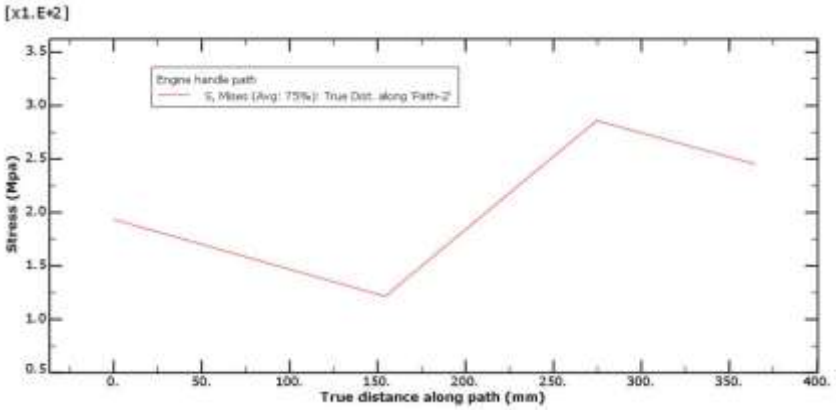

Figure 10. Contour Path of the Von Mises Stress Analysis in the Motor Mounts of the Structure.

Figure 11 shows the displacement contour of the DETSS. This figure shows the maximum displacement in the holders and radiator plates, ranging between 1.20 mm and 1.68 mm. The minimum displacement occurs in the battery holder, control panel, and structure plates along the y-axis direction, ranging between 0.24 mm and 0.96 mm.

Figure 12 shows the shear stress contour in the structure's XY direction (S12). The highest levels of shear stress are observed in the telescopic areas, radiator plates, part of the tank, a section of the battery holder, and the transverse steel part of the structure, ranging from 16 MPa to 68.2 MPa. The lowest shear stress occurs in the longitudinal chassis, the control panel assembly, the outer part of the battery holder frame, and parts of the tank, ranging from 0 MPa to -16 MPa.

The static analysis results indicate that the newly designed test stand is capable of achieving stress and displacement distribution in a way that enhances the accuracy of key diesel engine parameter measurements. These findings are consistent with the research by (Lloyd & Cackette, 2001; Qi et al., 2023), which emphasized improvements in measurement accuracy for engine testing. However, unlike (Voigt, 1991), which focused more on increasing control in engine testing systems, our design emphasizes improved safety and reduced testing time. This difference may be due to the incorporation of real-time diagnostic systems in the new design, contributing to more precise results.

Additionally, under certain high-load conditions, the stress distribution shows areas of stress concentration at specific points in the structure, likely due to the current design limitations. These findings suggest that further design improvements could lead to better stress distribution and extended structural lifespan. For future research, it is recommended to address these limitations and make design adjustments to reduce stress concentration.

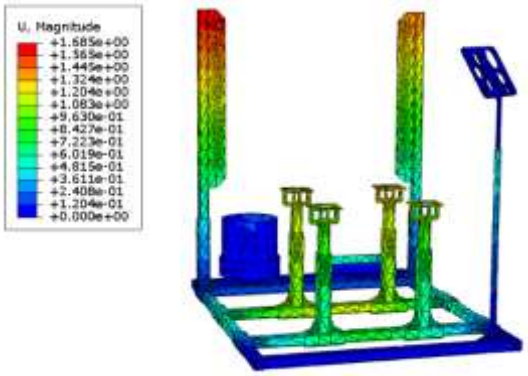

Figure 11. Displacement Contour in the DETSS.

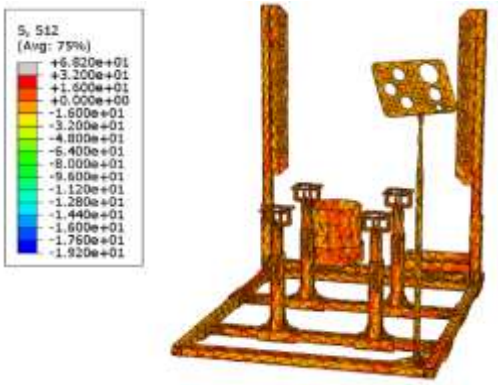

Figure 12. Shear Stress Contour in the X-Y Direction (S12) in the DETSS.

Results of the Modal Analysis of the DETSS

In the modal analysis of the DETSS, due to the engine startup and resulting vibrations, the vibration amplitudes occurred as shown in Figures 13-a (Mode 1) and 13-b (Mode 2) with frequencies of 1.87 Hz and displacement of 0.05 mm for the radiator mounts, and a frequency of 7.20 Hz with a displacement of 0.08 mm for the two motor mounts near the radiator. In Figures 14-a (Mode 3) and 14-b (Mode 4), the respective frequencies are 8.36 Hz with a displacement of 0.07 mm related to the motor mounts and tank, and 9.45 Hz with a displacement of 0.05 mm for the motor mounts, two longitudinal beams of the structure base, the fuel tank, and the control panel. In Figures 15-a (Mode 5) and 15-b (Mode 6), the respective frequencies are 10 Hz with a displacement of 0.05 mm related to the motor mounts and two transverse beams of the structure base and a frequency of 11 Hz with a displacement of 0.05 mm for the battery holder, tank, motor mounts, and two transverse beams of the structure base. Table 3 shows the frequency values in Hz and the displacement values of different DETSS components.

(a) (b)

Figure 13. a) Mode 1, b) Mode 2 in the Modal Analysis of the DETSS due to Engine Vibration.

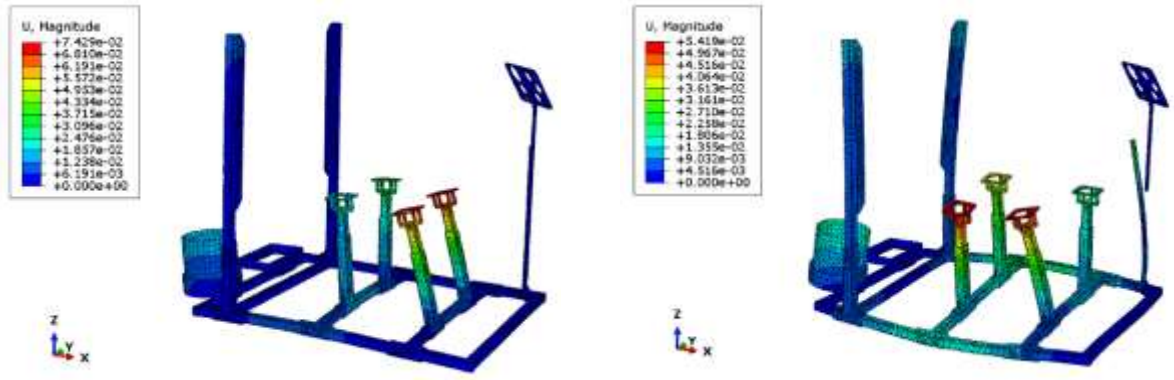

(a) **(b)**

Figure 14. a) Mode 3, b) Mode 4 in the Modal Analysis of the DETSS due to Engine Vibration.

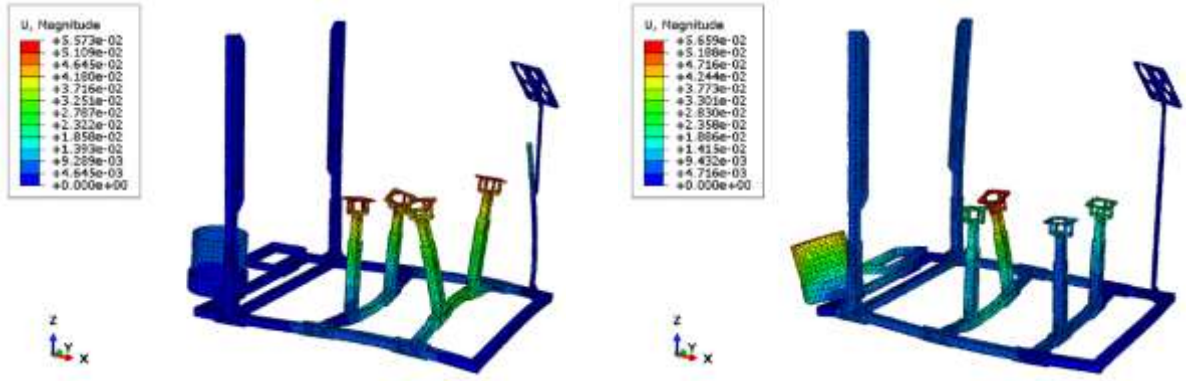

(a) **(b)**

Figure 15. a) Mode 5, b) Mode 6 in the Modal Analysis of the DETSS due to Engine Vibration.

Table 3. Frequency Values in Hertz and Displacement Values of Various Components in Millimeters.

Member No.	Mode No.	Displacement value (mm)	Frequency (HZ)
Member 1	First	0.05	1.87
Member 2	Second	0.08	7.20
Member 3	Third	0.07	8.36
Member 4	Fourth	0.05	9.45
Member 5	Fifth	0.05	10
Member 6	Sixth	0.05	11

Transverse Vibrations Due to Engine Dynamics on the DETSS

Transverse vibrations caused by engine dynamics are transmitted to the structural components. The displacement and time values for each structural component vary accordingly. The waveform used in the dynamic-vibrational analysis of the engine on the structure is a sinusoidal displacement amplitude (sin). Figure 16 shows the time-frequency and displacement values graph. The displacement values (U) in millimeters and time (T) in seconds are matched based on X-Y DATA and the analysis of the vibrational outputs of the structure. The natural frequencies, forcing frequencies, and mode shapes of the DETSS were extracted using the

frequency solver in ABAQUS software, utilizing the Lanczos method (Khennane, 2013).

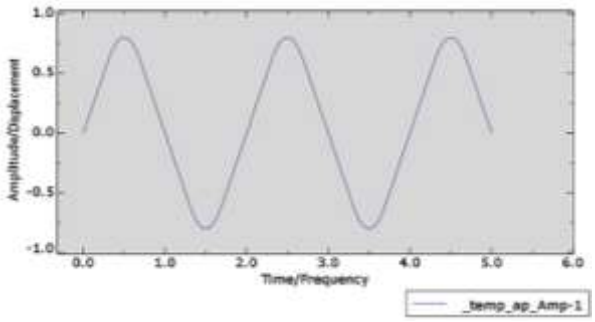

Figure 16. Time-Frequency and Sinusoidal Displacement-Amplitude Graph in ABAQUS Software.

Transverse Vibrations of Member 2 (Motor Mount Holder)

Figure 17 shows the displacement contour of the motor mount holder due to the dynamics of the diesel engine. According to this figure, the maximum displacement is 0.54 micrometers, and the minimum is 0.04 micrometers at 45 seconds, occurring periodically with sinusoidal vibrational waves. As shown in Figure 18, the maximum displacement of the motor mount holder due to the dynamics of the diesel engine occurs at 31, 30, 18, 11, and 3 seconds, with a value of 0.1 millimeters. The minimum displacement occurs at 7, 18, and 22 seconds, with values ranging from -0.05 to -0.1 millimeters.

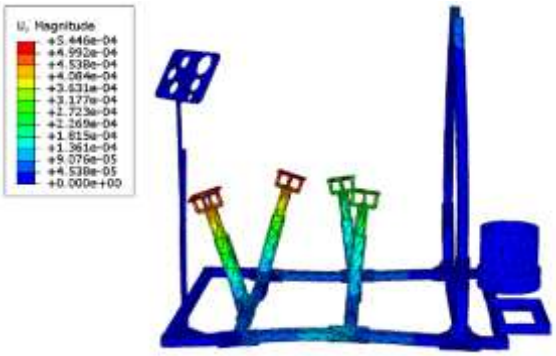

Figure 17. Displacement of the Contour of the Motor Mount Holder Due to Diesel Engine Dynamics.

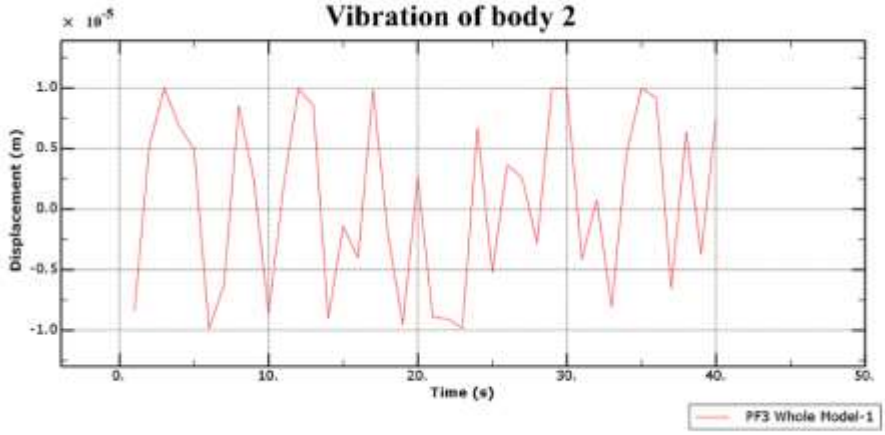

Figure 18. Transverse Vibration of Member 2 (Motor Mount Holder) Due to Engine Dynamics.

CONCLUSIONS

In this study, static and dynamic-vibrational analysis using the FEM was performed to examine stress-strain and modal analysis in the DETSS, and the following results were obtained:

- The studies indicated that the maximum von Mises stress was observed in the telescopic motor mount holders, as well as in the longitudinal and transverse frames of the structure, with values ranging from 300 to 617 MPa. Additionally, the minimum von Mises stress was observed in the radiator holders, fuel tank, and control panel, ranging from 100 to 175 MPa.
- The results of the vibrational analysis and modal analysis also indicated that the maximum displacement of 0.08 mm with a frequency of 7.20 Hz occurred in the areas of the longitudinal and transverse frames of the structure, motor mounts, and radiator holders. The minimum displacement of 0.05 mm with a frequency of 9.45 Hz was observed in the

control panel, fuel tank, and battery holder areas.

- In the study, the displacement of the structure in the X direction was almost zero. Thus, the maximum displacement of components in the Y direction ranged between 1.32 mm and 1.68 mm, while the minimum displacement ranged between 0.12 mm and 1.08 mm. Therefore, the initial structure needs to be reinforced and optimized based on the results. The reinforcement and optimization include strengthening key components of the structure, such as the motor mounts and radiator holder plates.

Funding: This research received no external funding.

Data Availability Statement: No data was used for the research described in the article.

Conflicts of Interest: The authors declare no conflict of interest.

REFERENCES

Altarazi, Y. S. M., Saadon, S., Yu, J., Gires, E., Ghafir, M. F. A., & Lucas, J. (2020). On-design operation and performance characteristic of custom engine. *Journal of Advanced Research in Fluid Mechanics and Thermal Sciences*, *70*(1), 144-154. https://doi.org/10.37934/arfmts.70.1.144154

Bogdan, D., Marek, W., Jozinkiewicz, D., Zakrzewski, S., Kaczmarek, M., Binkowski, D., . . . Krzysztof, S. (2023). Research of dynamic phenomena in a model engine stand. *Open Engineering*, *13*(1), 20220436. https://doi.org/10.1515/eng-2022-0436

Gholami, N., Afsari, A., Nazemosadat, S. M. R., & Afsari, M. J. (2023). Simulation and Dynamic-Thermal Analysis of Ceramic Disc and Brake Pad for Optimization by Finite Element Method. *International Journal of Advanced Design & Manufacturing Technology*, *16*(4), 9-22. https://doi.org/10.30486/admt.2024.1980467.1402

Homayounfar, H., & Amiri Chayjan, R. (2022). Simulation of Mass and Heat Transfer of Orange Slice during Drying Process under Vacuum Condition Using Finite Element Method. *Biomechanism and Bioenergy Research*, *1*(2), 51-55. https://doi.org/10.22103/BBR.2022.20484.1026

Khennane, A. (2013). *Introduction to finite element analysis using MATLAB® and abaqus*. CRC Press.

Lloyd, A. C., & Cackette, T. A. (2001). Diesel engines: environmental impact and control. *Journal of the Air & Waste Management Association*, *51*(6), 809-847. https://doi.org/10.1080/10473289.2001.10464315

Nazemosadat, S. M. R., Ghanbarian, D., Naderi-Boldaji, M., & Nematollahi, M. A. (2022). Structural analysis of a mounted moldboard plow using the finite element simulation method. *Spanish Journal of Agricultural Research*, *20*(2), e0204-e0204. https://doi.org/10.5424/sjar

Qi, Y., Liu, W., Liu, S., Wang, W., Peng, Y., & Wang, Z. (2023). A review on ammonia-hydrogen fueled internal combustion engines. *ETransportation*, *18*, 100288. https://doi.org/10.1016/j.etran.2023.100288

Reitz, R. D., Ogawa, H., Payri, R., Fansler, T., Kokjohn, S., Moriyoshi, Y., . . . Bae, C. (2020). IJER editorial: The future of the internal combustion engine. In (Vol. 21, pp. 3-10): SAGE Publications Sage UK: London, England.

Voigt, K. U. (1991). A control scheme for a dynamical combustion engine test stand. International Conference on IEE Control, Edinburgh, UK.